Microviscosity and temperature sensors: the twists and turns of the photophysics of conjugated porphyrin dimers

Aurimas Vyšniauskas[a,b] **and Marina K. Kuimova***[c]

[a]*Center of Physical Sciences and Technology, Sauletekio av. 3, Vilnius, LT-10257, Lithuania.*

[b]*Chemistry Department, Vilnius University, Naugarduko st. 24, Vilnius, LT-03225, Lithuania*

[c]*Chemistry Department, Imperial College London, Molecular Sciences Research Hub, White City Campus, Wood Lane, W12 0BZ, UK*

Received date (to be automatically inserted after your manuscript is submitted)
Accepted date (to be automatically inserted after your manuscript is accepted)

ABSTRACT: Conjugated porphyrin dimers have captured the imagination of scientists due to a set of unique spectroscopic features, such as remarkable nonlinear-optical properties, high yields of singlet oxygen sensitisation, the absorption and emission in the far-red region of the visible spectrum. Here we review a range of newly emerged applications of porphyrin dimers as sensors of their microenvironment, such as viscosity and temperature. We discuss the sensing mechanism based on the known conformational flexibility of the dimer structure and describe possible applications of these unique sensors, from detecting viscosity increase during photoinduced cell death to structural responses of polymers and artificial lipid membranes, to temperature changes, and to mechanical deformation.

KEYWORDS: porphyrin dimer, molecular rotors, temperature sensors, fluorescence spectroscopy, fluorescence lifetime imaging (FLIM)

*Correspondence to: Chemistry Department, Imperial College London, Molecular Sciences Research Hub, White City Campus, Wood Lane, W12 0BZ, UK. E-mail: m.kuimova@imperial.ac.uk.

INTRODUCTION

Porphyrinoids are a wide group of organic macrocycles that can be both natural and synthetic. Many porphyrinoids occur naturally and are crucial for performing important functions in living organisms [1], whereas synthetic porphyrins enjoy a large number of applications in many areas, for example, as sensitisers of singlet molecular oxygen [2], components of dye-sensitised solar cells [3], dyes for ion sensing [4], for magnetic resonance imaging (MRI) [5], and also for catalysis [6]. A porphyrin core presents a useful template for harvesting nonlinear-optical (NLO) properties [7] that can be exploited in multiphoton fluorescence microscopy [8], second harmonic generation (SHG) imaging [9] and in nonlinear multiphoton photodynamic therapy (PDT) that can be initiated with near-infrared ultrafast light pulses [10]. Conjugated porphyrin dimers (Scheme 1) emerged as a unique class of materials in possession of superior NLO properties [11,12]. Here we review another exciting property of these molecules, more recently discovered, which relates to conformational flexibility of their core: their ability to act as fluorescent sensors for microviscosity [13] and temperature [14,15] of their immediate environment. We analyse how this sensing capability, together with their ability to sensitise singlet oxygen [16] and their large two-photon absorption (TPA) cross-sections [17], make porphyrin dimers a truly unique class of useful materials. We analyse the mechanism of their function as sensors in a framework of photophysical and theoretical studies that explain the origins behind their unique nonlinear-optical properties and their conformational flexibility.

DISCUSSION

One and two-photon absorption properties of porphyrin dimers

Conjugated porphyrin dimers, where the porphyrin rings are connected by a butadiyne bridge, were first synthesised by Arnold and colleagues [18]. 15 years later, a set of porphyrin oligomers was synthesised and characterised by Anderson and co-workers, with the hope that a high third-order nonlinear susceptibility will enable their use as NLO materials [11,19]. This, indeed, has been shown to be the case, since it was discovered that porphyrin dimers possess extremely large TPA cross-sections exceeding 10 000 Göppert-Meyer units (GM) [17,20,21]. These high TPA cross-section values represent a remarkable achievement, given 1-100 GM is an expected value for a monomeric fluorophore, without specially incorporated design features for increased NL properties [22]. Additionally, porphyrin dimers and trimers connected *via* ethyne or butadiyne bridges were synthesised by Therien and co-workers as biomimetic materials with spectroscopic properties resembling those of a chloroplast [12].

A number of interesting spectroscopic signatures is characteristic of a conjugated dimer molecule, where two porphyrin chromophores are connected by an unsaturated bridge. The absorption spectra of such a dimer still feature the Q and Soret bands, expected in a monomeric porphyrin [23], but subtle changes occur (Figure 1A). A conjugation length is significantly extended in porphyrin dimers, which reduces a HOMO-LUMO gap and results in a redshift of the Q band [24]. The increased conjugation length also results in an increase in the oscillator strength for the transition in the Q band, leading to an increased absorption in the red compared to a monomeric porphyrin, a desirable property for a range of biological applications. Another contributing factor to the increased intensity of absorption in the red is that the Q band transition is no longer quasi-forbidden in the porphyrin dimer [25]. Notably, the Soret band becomes significantly broader [19]. The origin of broadening is the interaction between two transition dipole moments, which belong to each separate porphyrin ring,

according to the Kasha's point dipole approximation [26]. Since porphyrin dimers have a significant degree of flexibility, enabling rotation of the porphyrin rings relative to each other, the excitonic coupling between the transition dipole moments is different for each ring orientation, characterised by a dihedral angle, and this interaction produces slightly different excitation energies. The recorded absorption spectrum of a dimer is a sum of the spectra of the conformations with all possible dihedral angles (Figure 1C), which results in a broadened Soret band. The extent of both electronic and excitonic coupling between porphyrin rings depends on the position of the connecting bridge. It is the strongest for a *meso*-to-*meso* bridge (Scheme 1A, B), since both the HOMO and the LUMO of a porphyrin has a significantly higher probability density in the *meso* position, as compared to a β analogue [24].

One of the extremely attractive optical properties of the porphyrin dimers is their exceptionally high TPA cross sections, exceeding 10 000 GM. This unique property has been extensively explored in several works by Drobizhev *et al.* [17,25] and summarised in a review by Anderson and colleagues [27]. The TPA cross section for a butadiyne-linked dimer with no further substituents that can extend its conjugation is the highest for an excitation wavelength of around 850 nm, which means that the final excited state after TPA belongs to the Soret absorption band [17]. In order to fully explain the origins of high TPA cross section, σ_{TPA}, several factors need to be considered. Namely, *(i)* the resonance enhancement, *i.e.* the energy of the virtual state (equivalent to the energy of a TPA photon) is close in energy to an existing state, a Q band in a porphyrin dimer (Figure 2); *(ii)* an increased conjugation length in the porphyrin dimer, which makes a one photon Q transition allowed, leading to larger dipole moments (μ_{i0} and μ_{fi}, Figure 2), both enhancing σ_{TPA}; *(iii)* both transitions are polarised along the long molecular axis, thus maximising σ_{TPA}, all factors overall resulting in very impressive TPA cross sections [17,25].

Porphyrin dimers as PDT agents

Photodynamic Therapy (PDT) is a clinically useful treatment method for neoplastic diseases, such as cancer or age-related macular degeneration (AMD) [28]. During the treatment, a photosensitiser is localised specifically in malignant tissues, which is then selectively irradiated with an appropriate light source, to excite (or, in other words, activate) the photosensitiser. Following irradiation, the photosensitiser produces singlet oxygen, a reactive molecule which can oxidise unsaturated compounds within a cell and, thus, causes apoptosis or necrosis of a malignant cell. Porphyrins and porphyrinoids form one of the largest classes of PDT agents [29], due to their intense absorption in the red region of the spectrum (the so-called tissue transparency window, 650-950 nm [30], high yields of singlet oxygen production, and low dark toxicity to the healthy tissues.

Due to the dual selectivity of the treatment (preferential localisation of the photosensitiser into the tumor and its selective irradiation), PDT can selectively remove neoplastic tissues, while sparing healthy surrounding cells. A significantly higher degree of spatial localisation of PDT-induced damage can be achieved with a two-photon excitation (TPE), where the excitation probability is proportional to the square of the light intensity and, therefore, the photosensitiser is only excited in a focal volume of *ca* 1 μm^3. Near-infrared red light required for two-photon excitation of porphyrinoids falls into the tissue transparency window and is significantly less absorbed and scattered by tissues. Thus, TPE PDT is an attractive option for the treatment of conditions where the precise localisation of excitation in 3D in required, such as AMD (in the eye) [31,32], or 3D laser surgery, which might be beneficial in the patient's brain [33].

Thanks to their impressive TPA properties, porphyrin dimers and oligomers attracted significant attention as potential TPE PDT agents. Alike to monomeric porphyrins, porphyrin dimers have high quantum yields of singlet oxygen

sensitisation (> 50%) [34,35], although the yield decreases significantly for porphyrin tetramers and octamers [34]. One of the main challenges in designing porphyrin-based PDT agents is preventing their aggregation, leading to poor tissue/cellular delivery and poor photophysical properties, such as reduced quantum yields of singlet oxygen sensitisation and fluorescence [35]. A series of biocompatible porphyrin dimers with different charged substituents were synthesised by Balaz et al. (Chart 2) [36]. Water solubility was improved by using hydrophilic triethyleneglycol side groups and charged end groups, thus resulting in reduced aggregation. Ogawa and co-workers also investigated biocompatible porphyrin dimers connected *via* ethyne and butadiyne bridges as potential PDT agents [37]. All these molecules have large quantum yields of singlet oxygen sensitisation (50-90%) and TPA cross-sections exceeding 5 000 GM, and up to 17 000 GM for **P_2C_2-NMeI** (Chart 2) [35]. Moreover, their large extinction coefficients in linear (one-photon) absorption spectra (>10^5 $M^{-1}.cm^{-1}$) and red-shifted Q bands at > 650 nm also made them attractive as conventional one-photon PDT agents. The dimers with cationic end groups (**P_2-NMeI**, **P_2C_2-NMeI**, **P_2-NMe_3OAc**) were successfully internalised into cells, where they displayed good photostability [35] and low dark toxicity [38]. The photosensitiser with the highest PDT efficiency (**P_2C_2-NMeI**) was used to achieve a blood vessel closure in an *in vivo* mouse model (Figure 3) by using TPE PDT at 920 nm [39]. Despite these impressive results in an *in vivo* model, the TPE PDT, even when using porphyrin dimers as photosensitisers, is still deemed insufficiently efficient in an environment of the patient's eye, making it unsuitable for the treatment of AMD.

Conformational flexibility of porphyrin dimers

It may be expected that the most stable conformation of any conjugated porphyrin dimer, with respect to the dihedral angle between the porphyrin units, is its fully planar form, where the conjugation between the π orbitals is preserved along an entire molecule. However, as discussed above, there is a considerable conformational flexibility of the butadiyne-linked dimer along its central bond, as revealed by its absorption spectrum, Figure 1. Further evidence comes from the work by Tsuda *et al.,* investigating porphyrin dimers with pyridine substituents that form tetrameric box-shaped aggregates [40]. Their work demonstrated that butadiyne-linked porphyrin dimers form aggregates, in which the molecules are in a twisted, rather than a fully planar conformation, and the energy that is gained during aggregation is sufficient to compensate any energy loss resulting from the reduced conjugation in the twisted conformation. Early theoretical studies by Stranger *et al.*[41] and Lin *et al.*[24] have also shown that the ground state energy of a porphyrin dimer does not change significantly with respect to the dihedral angle between porphyrin rings. Furthermore, experimental studies of an ethyne-linked porphyrin dimer and trimer using transient absorption have indicated that the molecules can adopt multiple conformations in the ground state, however, if a non-planar conformer is excited, it planarises on a 30 ps time scale, at least in a non-viscous solvent dimethylformamide [42]. This unique conformational flexibility has enabled porphyrin dimers to be used both as a viscosity, tension and temperature sensors, *vide infra*.

The first detailed experimental and theoretical investigation into the conformational flexibility of porphyrin dimers was performed by Winters *et al.* [43] A bidentate dipyridil pyrrole ligand of a correct length was used, in order to bind to both metal centres in a dimer simultaneously, thus forcing it to adopt a planar conformation (Figure 4A). As the ligand was titrated into the solution of the porphyrin dimer, a marked change occurred in the absorption spectrum (Figure 4B): peaks at 490 nm and 740 nm increased, while peaks at 457 nm and 670 nm reduced. This change was assigned to the planarisation of the dimer upon the addition of the ligand, which allowed to assign the absorption peaks to the planar and the twisted forms of the dimer. These results further confirm that the dimer can adopt different conformations in the ground state, which have their own peaks in the absorption spectrum.

Furthermore, the emission spectrum of the dimer in a frozen glass matrix at 77K depended on the excitation wavelength: two emission peaks were observed, at 666 nm and 727 nm, when 457 nm excitation wavelength was used, however, the higher energy band at 666 nm was not present when excited at 490 nm. Therefore, the dimer in its non-planar form can be preferentially excited, which emits at 666 nm, whereas the planar form is excited at a lower energy, and no conversion to a higher energy twisted state is observed [43]. Time-resolved fluorescence decays of the same dimer upon 457 nm excitation in a frozen glass matrix have revealed that the decay recorded at 666 nm was fast, whereas the traces recorded at 727 nm had a rising component (the lifetime of which matched the decay time at 666 nm), followed by a slower decay. This data were interpreted as follows: when the porphyrin dimer was excited in its twisted form at the higher energy absorption peak, it rapidly planarised in the excited state, leading to dual emission, the fast decay at 666 nm, and a slower decay with a rise component at 727 nm. It should be noted that this interconversion could only be detected due to the rigidity of the frozen solvent matrix at 77 K; recall that the twisted to planar conversion of a structurally similar dimer in organic solvent at room temperature was complete by 30 ps [42], and such short lived species will not result in an additional emission band in a steady-state emission spectrum. A diagram detailing the interconversion between conformers is shown in Figure 5. Even though porphyrin dimers are likely to adopt a continuous range of conformations, spectroscopic data can be interpreted as the co-existence of two distinct species, which we designate as the planar and the twisted conformers.

Interconversion between conformers of porphyrin dimer was further experimentally investigated by Camargo *et al.* using two-dimensional electronic (2D ES) [44] and transient absorption [45] spectroscopies. In 2D ES experiment, it was possible to observe both 'twisted-to-planar' and 'planar-to-twisted' transitions in the ground state, but only the former was observed in the excited state. Using experimentally determined equilibrium constant between conformers in the ground state (K = 2.33) [46], time constants for 'twisted-to-planar' and 'planar-to-twisted' transitions have been experimentally determined to be 357 ps and 832 ps. In contrast, the time constant for 'twisted-to-planar' transition in the excited state has been found to be 62 ps in pentane. The authors also performed temperature-dependent transient absorption experiment in order to estimate the activation energy barrier for the conformational transition in the excited state. It was found to be 9.96 kJ/mol, although this value was heavily influenced by an increase in solvent viscosity at lower temperatures (*vide infra*), which means that the actual barrier is a lot smaller, probably similar to kT at room temperature. These results agree with temperature-dependent time-resolved fluorescence studies by Winters *et al.* in glassy 2-methyltetrahydrofuran at 77 K [43].

Theoretical work performed by Winters *et al.* [43] and Peeks *et al.* [46] confirms these experimental results and explains the appearance of two peaks in the absorption and emission spectra on the basis of the conformational dynamics of the dimers. The dependence of the calculated transition energies on the dihedral angle between porphyrin rings is shown in Figure 6, together with the oscillator strengths of these transitions. While in the B band no significant spectral changes occur, the Q band shifts to lower wavelength, with slightly decreased oscillator strength. However, there is a significant increase in the oscillator strength at 90° dihedral angle, which is one of the reasons that a pronounced additional peak appears at the blue edge of the Q band absorption, and an additional peak appears in the emission spectrum at around 650 nm (Figure 5B, C). The second factor that promotes the appearance of an extra peak in the spectra is a vibronic band of the planar conformer, predicted to appear at ~650 nm, coinciding with the twisted conformer band [46]. As a result of these two factors, both the absorption Q band and the emission spectrum appear to consist of two distinct peaks instead of displaying a broad featureless band.

The complex conformational dynamics of porphyrin dimers has important implications on their spectroscopic properties. For example, one of the most impressive properties of the conjugated dimers, their exceptionally high TPA cross section, is

strongly dependent on the conformation [47–49]. Ahn and colleagues have investigated a series of porphyrin dimers that range from being completely planar to significantly twisted, where porphyrin rings are connected by a single carbon-carbon bond [47]. This work demonstrated that a smaller dihedral angle between the porphyrin rings results in a larger TPA cross section. Additionally, experimental work by Wilkinson *et al.* on butadiyne-linked porphyrin dimer also demonstrated that the TPA cross section is dominated by the contribution from the planar conformer [49]. These results are supported by the theoretical work by Ohira and Bredas, showing that the TPA cross-section becomes vanishingly small when the dihedral angle approaches 90° [48].

The fluorescence quantum yields of singlet oxygen sensitisation, a parameter that is important for the function of the dimers as PDT agents [35,36,38,39], are also different for different conformers (Figure 7). A comparison between the 'excitation spectra' of singlet oxygen sensitisation and the excitation spectra of fluorescence for both conformers indicate that the twisted form is significantly less efficient at singlet oxygen production, in particular in a viscous environment, likely due to a faster intersystem crossing in the planar conformer, leading to high triplet yield, which is not observed in the twisted form [16]. The complexities resulting from the conformational flexibility, as detailed above, might seem as a disadvantage, however, we will describe that these properties enable porphyrin dimers to be used as unique sensors of microviscosity and temperature.

Viscosity sensitivity of porphyrin dimers

Given the relatively large size of porphyrin rings, it is not surprising that conformational transitions in porphyrin dimers are affected by the viscosity of the medium. We have established that the emission spectra of a butadiyne-bridged dimer **P_2C_2-NMeI** show a remarkable response to the viscosity of the solvent while being largely independent of the solvent polarity [13]. This allows to classify the conjugated porphyrin dimers as 'molecular rotors' [50,51]. Specifically, upon excitation into a 'twisted' absorption peak, the dimer showed dual emission, whereby the ratio of the twisted *vs* the planar conformers' emission was proportional to the viscosity of methanol/glycerol mixtures used as a solvent. The ratio was found to change as a function of viscosity in a power law, otherwise known as the Förster-Hoffmann equation, *i.e.* the data appear linear in a double logarithmic scale. In the case of the dimer **P_2C_2-NMeI**, the linearity in a double logarithmic plot was observed over three orders of magnitude, between 1-1000 cP [13]. Given the intrinsic biocompatibility of **P_2C_2-NMeI**, we have used ratiometric fluorescence imaging for sensing intracellular viscosity and found that the viscosity in a live cell is heterogeneous and exceeds 80 cP, a value considerably higher than that of an aqueous cytoplasm [52]. We then utilised the ability of the dimer to induce cellular apoptosis *via* singlet oxygen production [35,36,38,39], to measure changes in the intracellular viscosity upon photoinduced cell death (Figure 8) [13]. Our results showed that intracellular viscosity increases significantly during cell death, to *ca.* 300 cP (Figure 9C), a result that was corroborated by direct measurements of diffusion rates of formation and decay of singlet molecular oxygen in individual cells. Thus, the dimers were demonstrated to be dual agents, that can both induce PDT and cell death and quantitatively measure and image intracellular viscosity, by utilising their conformational flexibility. As previously noted, singlet oxygen production is significantly affected by the dimers' conformational flexibility, with the twisted conformer showing reduced singlet oxygen generation [16]. This property allows, in principle, to finely tune the dual functionality of the dimer: the irradiation in the 'planar' band mainly results in singlet oxygen generation and photoinduced cell death, while excitation into the 'twisted' peak mainly results in viscosity sensing. Such tuning is practical due to a limited ability of the twisted conformer to sensitise singlet oxygen, particularly in

a viscous environment such as cells; *e.g.* Figure 7A demonstrates very low singlet oxygen sensitisation at *ca.* 100 cP viscosity upon excitation between 445-485 nm, which is suitable for viscosity sensing [16].

Similarly, ethyne-bridged **PZn_2** has been employed by Kamat *et al.* for sensing membrane stress in polymersome membranes (Figure 9) [53]. This porphyrin dimer has a wide distribution of conformers in the ground state, different by a dihedral angle between the porphyrin rings, which becomes significantly narrower upon excitation, due to an increase in cumulenic character of the bridge, which forces the dimers to adopt a more planar conformation [54]. Such planar conformations are also favoured in confined, rigid environments. Since the planar conformer of **PZn_2** emits at a longer wavelength, the local tension of the membrane doped with this dye could be inferred from the position of the emission band of **PZn_2**. Thus, the ratiometric fluorescence measurements were performed in polymersomes that were degrading following an administration of a surfactant, or strained under micropipette aspiration, showing a clear change in rigidity of the porphyrin dimer's environment [53].

While ratiometric fluorescence imaging is a useful tool for viscosity sensing, it may be beneficial to have a dual readout, using at least two complementary methods. In the later work, we have shown that the butadiyne-bridged dimer **P_2-NMe_3OAc** can be used for dual-mode viscosity imaging, using both the ratiometric response and the time-resolved fluorescence decay of the twisted conformer, which are both viscosity-dependent (Figure 10) [55]. In this way, two independent maps of viscosity could be obtained, either *via* the ratiometric imaging or *via* Fluorescence Lifetime Imaging (FLIM). Both techniques had a good dynamic range of responses. Such dual imaging approach allowed for the verification of results of each individual method. For instance, it was found that ratiometric results cannot always be trusted due to the dye aggregation, which is not immediately obvious from the spectra. While aggregation was not expected from a biocompatible dimer such as **P_2-NMe_3OAc**, excited state quenching clearly manifested itself in significant changes to fluorescence lifetimes, recorded *via* FLIM in certain environments, e.g. self-assembly of **P_2-NMe_3OAc** on the surface of lipid bilayers in the aqueous phase.

Since porphyrin dimers are known to have a large TPA cross section, viscosity sensing upon two-photon excitation was also attempted in this work [55]. However, the twisted conformer needs to be excited to achieve viscosity sensing. Therefore, no viscosity-dependent emission was observed upon two-photon excitation, since the twisted conformer TPA is far weaker than that of its planar counterpart, as discussed in the previous section.

Various porphyrin dimers linked *via* butadiyne bridge have also been used for sensing the inner environment of polymers [56,57] and ionic liquids [58,59], *via* ratiometric or lifetime methods. Lee *et al.* have performed a single-molecule fluorescence experiment with porphyrin dimer incorporated in poly(methyl methaacrylate) (PMMA) films of varying density, from 5 to 50 mg/mL [56]. The single-molecule fluorescence intensity traces (FITs) have shown two types of photobleaching behaviour: it was either a one-step photobleaching (assigned to the planar conformer) or a two-step photobleaching (assigned to the twisted conformation, where the electronic coupling between two porphyrin rings is weak and they behave as two separate chromophores). In PMMA matrices of increasing density two-step photobleaching behaviour was more frequent, and fluorescence lifetime was shorter on average [56], which was consistent with a larger number of twisted conformers in a more dense and tightly packed polymer matrix [55]. The distribution of single molecule lifetimes from the dimers was the highest in the densest PMMA matrix, meaning that it contained the broadest distribution of conformers of the dimer. Doan and colleagues have investigated a porphyrin dimer in polymer films, but instead of changing the density of the film, they have studied changes in the emission spectra of a porphyrin dimer upon mechanical deformation (stretching) of the film [57]. They have shown that the emission peak that corresponds to the twisted conformer

becomes progressively weaker as the film is stretched. One possible explanation is that the environment of the dimer becomes less crowded as a result of the stretch, which results in a faster twisted-to-planar transition, following the initial excitation. Alternatively, the stretching of the film may force the porphyrin dimer to adopt more planar conformations, similarly to the ethyne-bridged dimer studied by Kamat *et al.* (Figure 9) [53]. The latter explanation is consistent with some of the temperature-dependent data reported in this work [57]. It will become clear from the following section that the temperature-dependent behaviour of porphyrin dimers is rather complex, and the explanation required to explain experimental data goes beyond a simple change of the environmental viscosity upon heating or cooling the solvent.

Porphyrin dimers can also be used for viscosity sensing in ionic liquids, as demonstrated by the work of Jameson *et al.* [58,59]. They have performed ratiometric measurements of viscosity in a set of ionic liquids that had three different inorganic anions and alkyl cations of different length [58]. Similarly, to what was previously found in viscous mixtures of standard organic solvents, porphyrin dimer **P_2C_2-NMeI** was shown to be sensitive to the viscosity of ionic liquids studied. However, the degree of sensitivity was significantly lower, *i.e.* ~10× a viscosity increase of an ionic liquid was required to achieve a similar ratiometric ratio increase as in organic solvent mixtures. Additionally, the degree of viscosity sensitivity was also affected by the nature of both an anion and a cation of the ionic liquids. This observation suggests, as stated by the authors, that the structure of ionic liquids is more important than its viscosity in determining the ratiometric response of **P_2C_2-NMeI** [58], pointing at specific fluorophore-liquid interactions. This is different to the mechanism of viscosity sensitivity in standard solvents, where a solvent free volume is hypothesised to influence the conformer interconversion [60].

Subsequent work has shown that the ratiometric response of porphyrin dimer can also be affected by confinement. When the dimer is confined in reverse micelles, it reports higher viscosity compared to being in a neat solvent. This was observed for both ionic liquid [C_4-mim]PF_6 and for an organic solvent dimethylsulfoxide (DMSO) [59].

In summary, porphyrin dimers represent a unique class of fluorescent viscosity sensors, with remarkably red-shifted absorption and fluorescence spectra between 600-800 nm, coinciding with the tissue transparency window [61]. One of their unique advantages is the ability to sense viscosity both ratiometrically, *vi*a spectral measurements of the twisted *vs* the planar emission peaks, as well as by the time-resolved fluorescence decay (*i.e*. the fluorescence lifetime), generally of a twisted conformer. While the instrumentation required for the time-resolved measurements of fluorescence is typically more complex, the ability to verify the measurement result by a dual readout makes porphyrin dimers a versatile and a reliable probe, suitable for quantitative measurements. However, it has been noted that even biocompatible dimers, decorated with solubilising groups, appear to be prone to aggregation in aqueous environments [55], which may interfere with their application for viscosity sensing in biological samples. In addition to introducing more water-solubilising groups, a possible way to circumvent this obstacle could be to investigate the behaviour of a free-base porphyrin dimer with no metal, which may be less likely to aggregate [19].

Temperature sensitivity of porphyrin dimers

It was discovered that butadiyne porphyrin dimers are not only sensitive to viscosity, but also temperature. Hammerer and colleagues were first to report this [14]. They have demonstrated that the glycosylated porphyrin dimer (Figure 11A) is able to sense the temperature of water ratiometrically. In this case, the effect of changing viscosity upon changes in temperature could be excluded, since the viscosity of water responds only slightly to temperature. When the temperature was increased, the emission from the twisted conformer increased, while the planar conformer emitted less light (Figure

12B). The exact temperature sensing mechanism was unclear but the authors hypothesised that it involves a change in hydrogen bonding, which affects both conformers differently at different temperatures.

In our own work, we demonstrated that for porphyrin dimer **P_2-NMe_3OAc** (Chart 2), the ratio of the twisted *vs* the planar emission peaks is sensitive only to viscosity but not to temperature. These measurements were performed in heated methanol/glycerol mixtures, where the same viscosity could be achieved by either changing the composition of the mixture or by changing the temperature. Our data showed a perfect overlap in fluorescent twisted/planar ratios, independent of the composition and the temperature of the mixture studied, as long as the mixtures had identical viscosity, Figure 12B. This means that the ratiometric viscosity sensing by the dimer **P_2-NMe_3OAc** was temperature-independent, enabling viscosity determination at varying temperature. At the same time, the fluorescence lifetime of the twisted conformer of the same dimer **P_2-NMe_3OAc** was found to be affected by both parameters [15], *i.e.* the lifetimes recorded at different compositions and temperatures (but at the same viscosity) did not overlap, Figure 12C. It was, however, possible to fit the lifetime data by using a modified version of a Förster-Hoffmann equation, which included an Arrhenius term, Figure 12D. It follows that it was possible to use that equation to determine the temperature of the mixture, from the measured lifetime and the known viscosity. Consequently, by combining ratiometric and lifetime measurements, it was possible to image both viscosity and temperature simultaneously, making **P_2-NMe_3Oac** the first dual temperature/viscosity probe reported.

Our later work investigated a series of porphyrin dimers with different end groups and revealed that these dyes have drastically different sensitivities to both viscosity and temperature [62]. For the dimer **P_2-NMeI** (Chart 2), characterised by a higher conjugation length, not only the twisted but also the planar conformer demonstrated sensitivity to both viscosity and temperature. Additionally, **P_2-NMeI** had a complementary dynamic range to **P_2-NMe_3Oac**, making it more suitable for lower temperature and higher viscosity measurements, as compared to **P_2-NMe_3OAc**. In comparison to the above two dimers, the ratiometric and the lifetime data for the dimer **P_2** (Chart 2), which had no charged end groups, was sensitive to viscosity only and not to temperature, making **P_2** a dimer of choice for viscosity-only dual mode probing in hydrophobic environments, where it has a good solubility. Overall, these results demonstrated that it was possible to tune viscosity- and temperature-sensitive properties of porphyrin dimers by subtle changes to their peripheral substituents. With many more conjugated porphyrin dimer structures available by possible future synthetic modification, including asymmetric structures, there is a large scope for creating superior probes of viscosity and temperature with unique spectroscopic properties, suitable for a particular environment of interest.

CONCLUSIONS AND OUTLOOK

Conjugated porphyrin dimers form a unique class of fluorophores with a remarkable set of useful spectroscopic properties. They can be excited in the so called ‘tissue optical window‘, and they emit light in the far red region of the visible spectrum, considerably more red-shifted compared to monomeric porphyrinoids. A number of dimers have extremely high TPA cross sections, exceeding the values of any other reported nonlinear absorbers, up to 17 000 GM. At the same time, the dimers are efficient sensitisers of singlet molecular oxygen, which makes them attractive second-generation sensitisers for one- and two-photon excited PDT, with significant absorption in the red region of the spectrum. It has recently become apparent that due to their unique conformational flexibility, they can be used as viscosity sensors, temperature sensors and even as dual viscosity-temperature sensors, simultaneously sensing both environmental parameters by combining spectral and time-resolved fluorescence responses.

As a result of this collection of properties, porphyrin dimers have been applied in a variety of tasks: as sensors of temperature and viscosity in bulk solvent mixtures, to probe microenvironment and packing in polymers in steady-state and upon mechanical deformation, in ionic liquids and as biocompatible sensitisers and probes for cellular environments. The latter includes sensitisers for one-photon and two-photon excited PDT, monitoring lipid packing in model membranes and in live biologiocal cells, and the changes in local viscosity during apoptosis and PDT. However, the potential of porphyrin dimers to be applied as quantitative sensors in biological systems is somewhat limited by their insufficient water solubility and their tendency to aggregate. The possibility of dual-mode environmental sensing (*e.g. via* the ratiometric detection and *via* fluorescence lifetimes) is, therefore, increasingly important, especially to enable quantitative conclusions, by independently verifying the results of both methods.

Though a number of unique properties of porphyrin dimers is already known, a significant number of yet undiscovered properties and new application avenues likely exist. The basic spectroscopic properties, the origins of high TPA cross-sections and the origin of conformational equilibrium of porphyrin dimers is significantly researched. However, the origins of their temperature sensitivity remain poorly understood. Theoretical studies into temperature-dependent properties of the dimers could not only explain the experimental observations for the already known molecules but will likely assist in creating new and superior dual viscosity/temperature probes, including those that are able to work in biological environment without the risk of aggregation.

The main body of work to date was focused on the porphyrin dimers incorporating a butadiyne bridge. Ethyne-bridged porphyrin dimers may have equally exciting sensory properties but, to our knowledge, there is only one report where such dyes were applied to viscosity sensing. A theoretical study of the ethyne-bridged dimer indicated that its viscosity-sensing mechanism may be different from the one for butadiyne-bridged dimers and may be similar to that of ‘fluorescent flippers‘ – a popular class of fluorophores used for measuring membrane tension.[63,64] Therefore, this class of dimers (as well as alternative bridge structures) may have significant potential for exciting and new applications, which have not yet been explored.

In conclusion, porphyrin dimers are an exciting class of fluorophores that have few rivals in terms of a number and a range of possible applications. While a significant body of work exists, investigating a wide range of their spectroscopic properties and applications, we have no doubt that these unique structures hold significant promise as useful molecular tools for the future, to scientists working in many different areas of biology, physics, chemistry and other molecular sciences.

REFERENCES

1. Meinschein WG, Barghoorn ES and Schopf JW. *Science* 1964; **145**: 262 LP - 263.
2. Ackroyd R, Kelty C, Brown N and Reed M. *Photochem. Photobiol.* 2001; **74**: 656-669.
3. Birel Ö, Nadeem S and Duman H. *J. Fluoresc.* 2017; **27**: 1075-1085.
4. Ding Y, Zhu W-H and Xie Y. *Chem. Rev.* 2017; **117**: 2203-2256.
5. Imran M, Ramzan M, Qureshi AK, Azhar Khan M and Tariq M. *Biosensors* 2018; **8**: 1-17.
6. Zhang W, Lai W and Cao R. *Chem. Rev.* 2017; **117**: 3717-3797.

7. Senge MO, Fazekas M, Notaras EGA, Blau WJ, Zawadzka M, Locos OB and Mhuircheartaigh EMN. *Adv. Mater.* 2007; **19**: 2737-2774.
8. Kim D, Ryu HG and Ahn KH. *Org. Biomol. Chem.* 2014; **12**: 4550-4566.
9. Pantazis P, Maloney J, Wu D and Fraser SE. *Proc. Natl. Acad. Sci. U. S. A.* 2010; **107**: 14535-14540.
10. Sun Z, Zhang LP, Wu F and Zhao Y. *Adv. Funct. Mater.* 2017; **27**: 1-21.
11. Anderson HL, Martin SJ and Bradley DDC. *Angew. Chem. Int. Ed.* 1994; **33**: 655-657.
12. Lin VS, DiMagno SG and Therien MJ. *Science* 1994; **264**: 1105-1111.
13. Kuimova MK, Botchway SW, Parker AW, Balaz M, Collins HA, Anderson HL, Suhling K and Ogilby PR. *Nat. Chem.* 2009; **1**: 69-73.
14. Hammerer F, Garcia G, Charles P, Sourdon A, Achelle S, Teulade-Fichou M-P and Maillard P. *Chem. Commun.* 2014; **50**: 9529-9532.
15. Vyšniauskas A, Qurashi M, Gallop N, Balaz M, Anderson HL and Kuimova MK. *Chem. Sci.* 2015; **6**: 5773-5778.
16. Kuimova MK, Balaz M, Anderson HL and Ogilby PR. *J. Am. Chem. Soc.* 2009; **131**: 7948-7949.
17. Drobizhev M, Stepanenko Y, Dzenis Y, Karotki A, Rebane A, Taylor PN and Anderson HL. *J. Am. Chem. Soc.* 2004; **126**: 15352-15353.
18. Arnold DP, Johnson AW and Mahendran M. *J. Chem. Soc. Perkin Trans. 1* 1978: 366-370.
19. Anderson HL. *Inorg. Chem.* 1994; **33**: 972-981.
20. Ogawa K, Ohashi A, Kobuke Y, Kamada K and Ohta K. *J. Am. Chem. Soc.* 2003; **125**: 13356-13357.
21. Karotki A, Drobizhev M, Dzenis Y, Taylor PN, Anderson HL and Rebane A. *Phys. Chem. Chem. Phys.* 2004; **6**: 7-10.
22. Xu C and Webb WW. *J. Opt. Soc. Am. B* 1996; **13**: 481-491.
23. Gouterman M. *J. Mol. Spectrosc.* 1961; **6**: 138-163.
24. Lin VSY and Therien MJ. *Chem. - A Eur. J.* 1995; **1**: 645-651.
25. Drobizhev M, Stepanenko Y, Dzenis Y, Karotki A, Rebane A, Taylor PN and Anderson HL. *J. Phys. Chem. B* 2005; **109**: 7223-7236.
26. M K, R RH and M AE-B. *Pure Appl. Chem.* 1965; **11**: 371.
27. Pawlicki M, Collins HA, Denning RG and Anderson HL. *Angew. Chem. Int. Ed.* 2009; **48**: 3244-3266.
28. Ochsner M. *J. Photochem. Photobiol. B Biol.* 1997; **39**: 1-18.
29. Kou J, Dou D and Yang L. *Oncotarget* 2017; **8**: 81591-81603.
30. Weissleder R. *Nat. Biotechnol.* 2001; **19**: 316-317.
31. Arnold J, Barbezetto I, Birngruber R, Bressler NM, Bressler SB, Donati G, Fish GE, Flaxel CJ, Gragoudas ES, Harvey P, Kaiser PK, Koester JM, Lewis H, Lim JI, Ma C, Meredith TA, Miller JW, Mones J, Murphy SA, Pieramici DJ, Potter MJ, Reaves A, Rosenfeld PJ, Schachat AP, Schmidt-Erfurth U, Singerman L, Strong HA, Stur M and Williams GA. *Am. J. Ophthalmol.* 2001; **131**: 541-560.
32. Chen B, Pogue BW, Hoopes PJ and Hasan T. *Crit. Rev. Eukaryot. Gene Expr.* 2006; **16**: 279-306.
33. Yanik MF, Cinar H, Cinar HN, Chisholm AD, Jin Y and Ben-Yakar A. *Nature* 2004; **432**: 822.
34. Kuimova MK, Hoffmann M, Winters MU, Eng M, Balaz M, Clark IP, Collins HA, Tavender SM, Wilson CJ, Albinsson B, Anderson HL, Parker AW and Phillips D. *Photochem. Photobiol. Sci.* 2007; **6**: 675-682.
35. Kuimova MK, Collins HA, Balaz M, Dahlstedt E, Levitt JA, Sergent N, Suhling K, Drobizhev M, Makarov NS,

Rebane A, Anderson HL and Phillips D. *Org. Biomol. Chem.* 2009; **7**: 889-896.

36. Balaz M, Collins HA, Dahlstedt E and Anderson HL. *Org. Biomol. Chem.* 2009; **7**: 874-888.
37. Ogawa K, Hasegawa H, Inaba Y, Kobuke Y, Inouye H, Kanemitsu Y, Kohno E, Hirano T, Ogura SI and Okura I. *J. Med. Chem.* 2006; **49**: 2276-2283.
38. Dahlstedt E, Collins HA, Balaz M, Kuimova MK, Khurana M, Wilson BC, Phillips D and Anderson HL. *Org. Biomol. Chem.* 2009; **7**: 897-904.
39. Collins HA, Khurana M, Moriyama EH, Mariampillai A, Dahlstedt E, Balaz M, Kuimova MK, Drobizhev M, Yang VXD, Phillips D, Rebane A, Wilson BC and Anderson HL. *Nat. Photonics* 2008; **2**: 420-424.
40. Tsuda A, Hu H, Tanaka R and Aida T. *Angew. Chem. Int. Ed.* 2005; **44**: 4884-4888.
41. Stranger R, McGrady JE, Arnold DP, Lane I and Heath GA. *Inorg. Chem.* 1996; **35**: 7791-7797.
42. Kumble R, Palese S, Lin VSY, Therien MJ and Hochstrasser RM. *J. Am. Chem. Soc.* 1998; **120**: 11489-11498.
43. Winters MU, Karnbratt J, Eng M, Wilson CJ, Anderson HL and Albinsson B. *J. Phys. Chem. C* 2007; **111**: 7192-7199.
44. Camargo FVA, Anderson HL, Meech SR and Heisler IA. *J. Phys. Chem. B* 2015; **119**: 14660-14667.
45. Camargo FVA, Hall CR, Anderson HL, Meech SR, Heisler IA, Camargo FVA, Hall CR and Anderson HL. *Struct. Dyn.* 2016; **3**: 1-12.
46. Peeks MD, Neuhaus P and Anderson HL. *Phys. Chem. Chem. Phys.* 2016; **18**: 5264-5274.
47. Ahn TK, Kim KS, Kim DY, Noh SB, Aratani N, Ikeda C, Osuka A and Kim D. *J. Am. Chem. Soc.* 2006; **128**: 1700-1704.
48. Ohira S and Bredas JL. *J. Mater. Chem.* 2009; **19**: 7545-7550.
49. Wilkinson JD, Wicks G, Nowak-Król A, Łukasiewicz ŁG, Wilson CJ, Drobizhev M, Rebane A, Gryko DT and Anderson HL. *J. Mater. Chem. C* 2014; **2**: 6802-6809.
50. Kuimova MK. *Phys. Chem. Chem. Phys.* 2012; **14**: 12671-12686.
51. Vyšniauskas A and Kuimova MK. *Int. Rev. Phys. Chem.* 2018; **37**: 259-285.
52. Luby-Phelps K, Mujumdar S, Mujumdar RB, Ernst LA, Galbraith W and Waggoner AS. *Biophys. J.* 1993; **65**: 236-242.
53. Kamat NP, Liao ZZ, Moses LE, Rawson J, Therien MJ, Dmochowski IJ and Hammer DA. *Proc. Natl. Acad. Sci. U. S. A.* 2011; **108**: 13984-13989.
54. Rubtsov I V., Susumu K, Rubtsov GI and Therien MJ. *J. Am. Chem. Soc.* 2003; **125**: 2687-2696.
55. Vyšniauskas A, Balaz M, Anderson HL and Kuimova MK. *Phys. Chem. Chem. Phys.* 2015; **17**: 7548-7554.
56. Lee JE, Yang J and Kim D. *Faraday Discuss.* 2012; **155**: 277-288.
57. Doan H, Raut SL, Yale D, Balaz M, Dzyuba S V. and Gryczynski Z. *Chem. Commun.* 2016; **52**: 9510-9513.
58. Jameson LP, Kimball JD, Gryczynski Z, Balaz M and Dzyuba S V. *RSC Adv.* 2013; **3**: 18300-18304.
59. Jameson LP, Balaz M, Dzyuba S V. and Kamiya N. *RSC Adv.* 2014; **4**: 705-708.
60. Loufty RO and Arnold BA. *J. Phys. Chem.* 1982; **86**: 4205-4211.
61. Weissleder R. *Nat. Biotechnol.* 2001; **19**: 316-317.
62. Vyšniauskas A, Ding D, Qurashi M, Boczarow I, Balaz M, Anderson HL and Kuimova MK. *Chem. - A Eur. J.* 2017; **23**: 11001-11010.
63. Dal Molin M, Verolet Q, Colom A, Letrun R, Derivery E, Gonzalez-Gaitan M, Vauthey E, Roux A, Sakai N and

Matile S. *J. Am. Chem. Soc.* 2015; **137**: 568-571.

64. Strakova K, Assies L, Goujon A, Piazzolla F, Humeniuk H V and Matile S. *Chem. Rev.* 2019; **119**: 10977-11005.

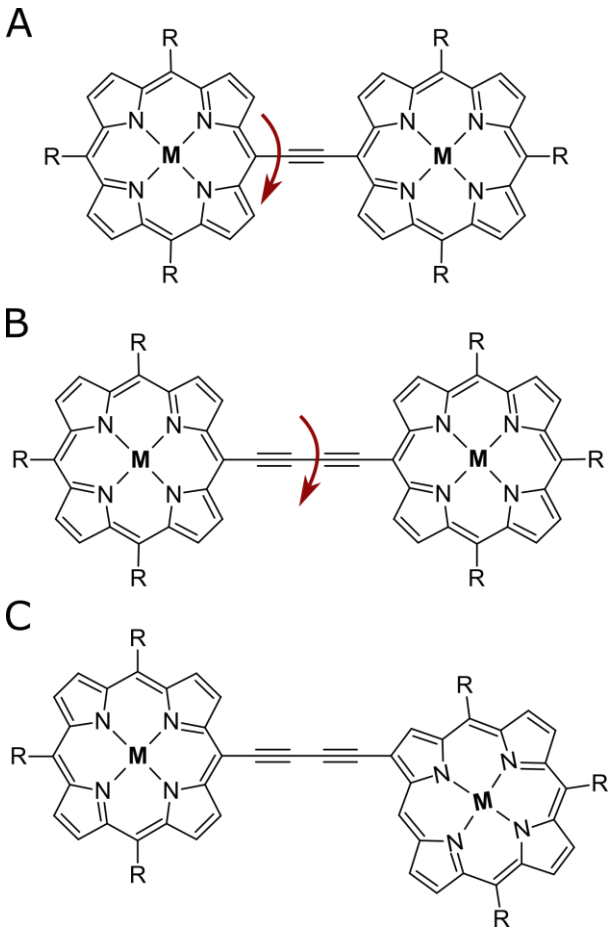

Chart 1. Molecular structures of porphyrin dimers with ethyne (A) and butadiyne (B) bridges. Porphyrin dimer with a butadiyne bridge connecting carbon atoms in *meso* positions is shown in (B), whereas (C) shows a dimer with a *meso-β* bridge. **M** is a metal ion which may or may not be present. The red arrows highlight the conformational flexibility of porphyrin dimers.

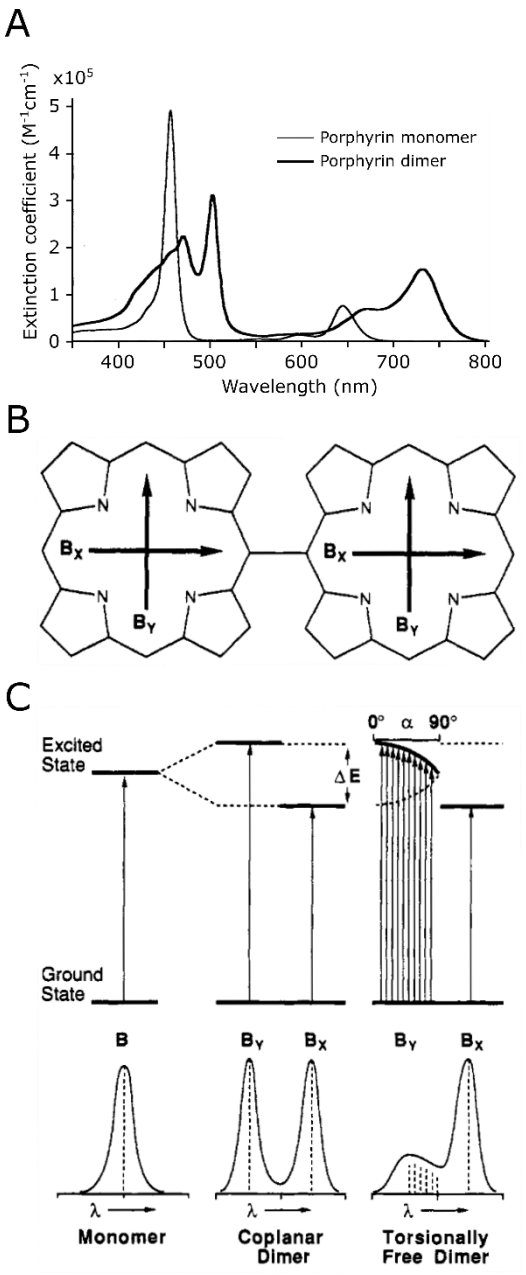

Figure 1. A) Absorption spectra of porphyrin monomer (thin line) and dimer with a butadiyne bridge (thick line). B) Transition dipoles giving rise to the Soret band. C) Energy diagrams for porphyrin monomer, dimer in the coplanar conformation, and for a torsionally free dimer. The lower panel shows the shape of the Soret band expected for each scenario. Adapted with permission from Anderson HL. *Inorg. Chem.* 1994; **33**: 972-981. Copyright 1994 American Chemical Society.

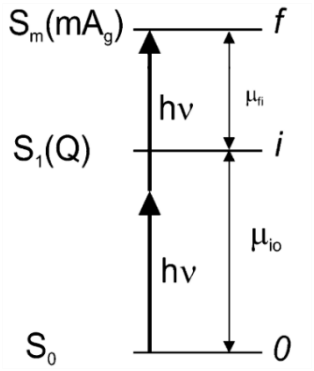

Figure 2. Three electronic states participating in TPA of a porphyrin dimer. *0* is the initial state, *i* is the intermediate state, transition to which is one-photon allowed (the Q band), whereas *f* is the final two-photon allowed state with the A_g symmetry. Adapted with permission from Drobizhev M, Stepanenko Y, Dzenis Y, Karotki A, Rebane A, Taylor PN and Anderson HL. *J. Phys. Chem. B* 2005; **109**: 7223-7236. Copyright 2005 American Chemical Society.

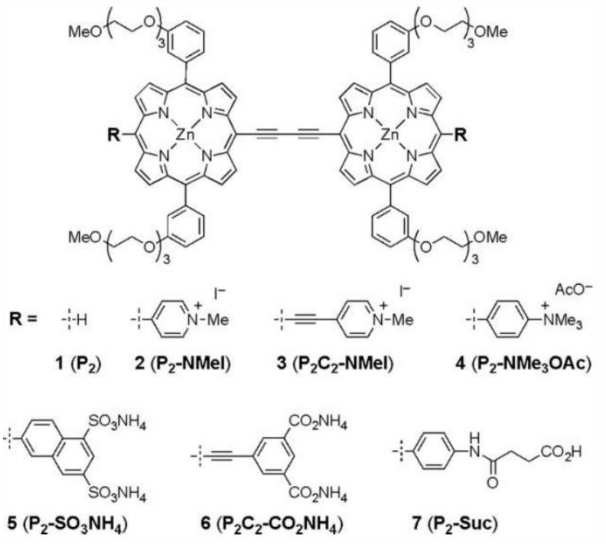

Chart 2. Molecular structures of porphyrin dimers designed for use as PDT agents in live cells. Reproduced from Ref. 34 with permission from The Royal Society of Chemistry.

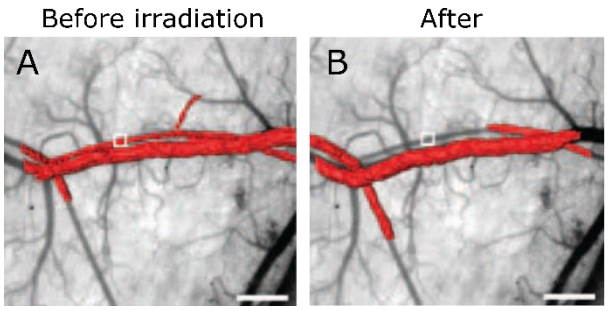

Figure 3. Doppler optical coherence tomography images of blood vessels of a mouse (window chamber model) showing blood flow before (A) and after (B) TPE PDT treatment using **P_2C_2-NMeI**. After the treatment, the blood flow is stopped in a blood vessel marked by a white rectangle (the area irradiated with two photon light at 920 nm), without affecting the neighbouring blood vessel. The scale bar is 400 μm. The figure is adapted from ref.[39] with permission.

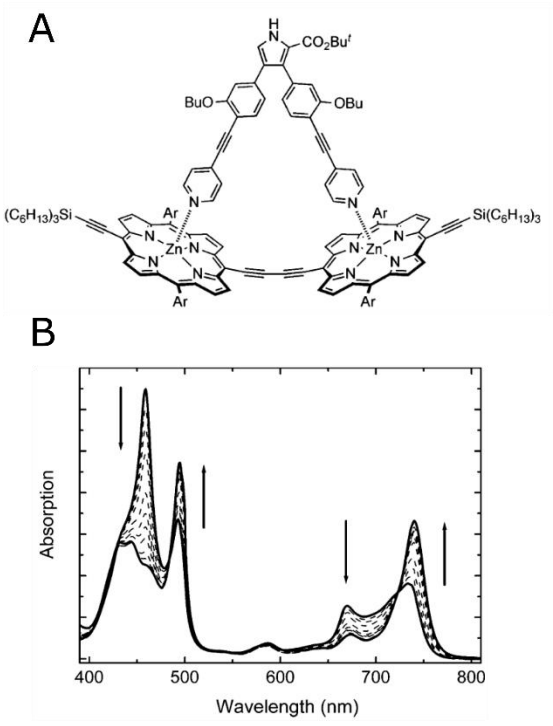

Figure 4. A) A structure of the porphyrin dimer examined in the work of Winters *et al.* together with a bidentate dipyridil pyrrole ligand that was used to fix the dimer in its planar conformation. B) The changes in the absorption spectrum that occur upon titration of the ligand shown in A). Adapted with permission from Winters MU, Karnbratt J, Eng M, Wilson CJ, Anderson HL and Albinsson B. *J. Phys. Chem. C* 2007; **111**: 7192-7199. Copyright 2007 American Chemical Society.

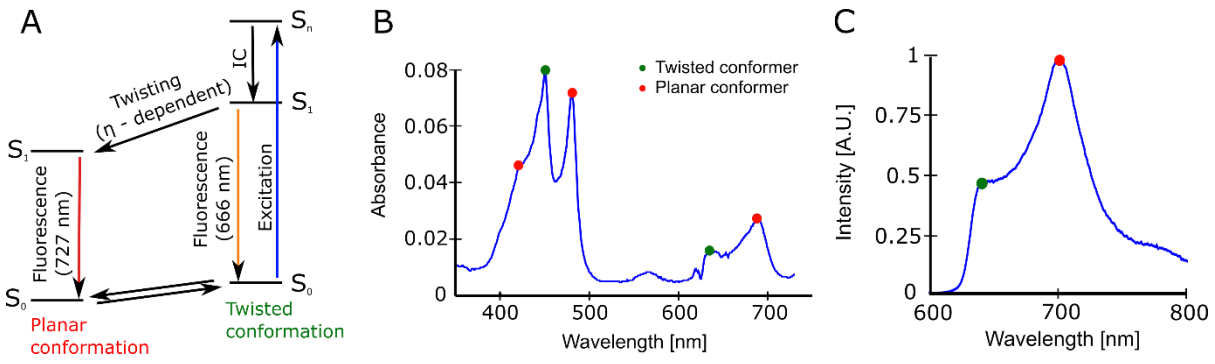

Figure 5. A) An energy level diagram for butadiyne bridged porphyrin dimers, demonstrating the interplay between the twisted and the planar conformers, in the ground and the excited states. In the ground state, both conformers interconvert freely (low energy barrier), whereas in the excited state only the 'twisted-to-planar' transition is possible. IC – internal conversion. B, C) Absorption (B) and fluorescence (C) spectra of a typical porphyrin dimer. Each peak is assigned to either the planar or the twisted conformer. Reproduced from Ref. 54 with permission from the PCCP Owner Societies.

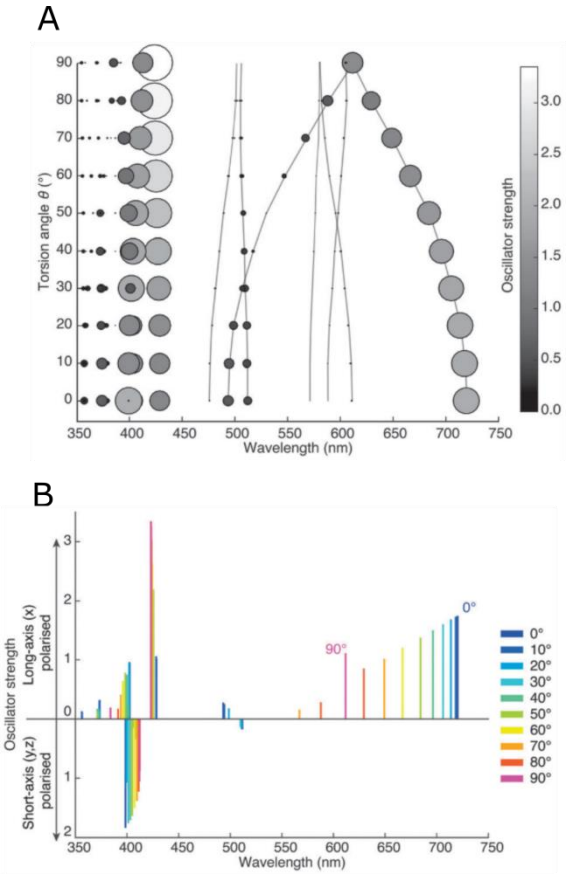

Figure 6. A) Calculated absorption wavelengths corresponding to individual transitions between the ground state and the excited states of a butadiyne bridged porphyrin dimer with respect to the dihedral angle between the porphyrin rings. The oscillator strength of the transitions is denoted by the colour of the circles. B) Calculated transition energies with respect to the oscillator strengths for dihedral angles 0° to 90°. Position of the bars denote whether the corresponding transition is polarised parallel or perpendicular to the long axis of the porphyrin dimer. Reproduced from Ref. 45 with permission from the PCCP Owner Societies.

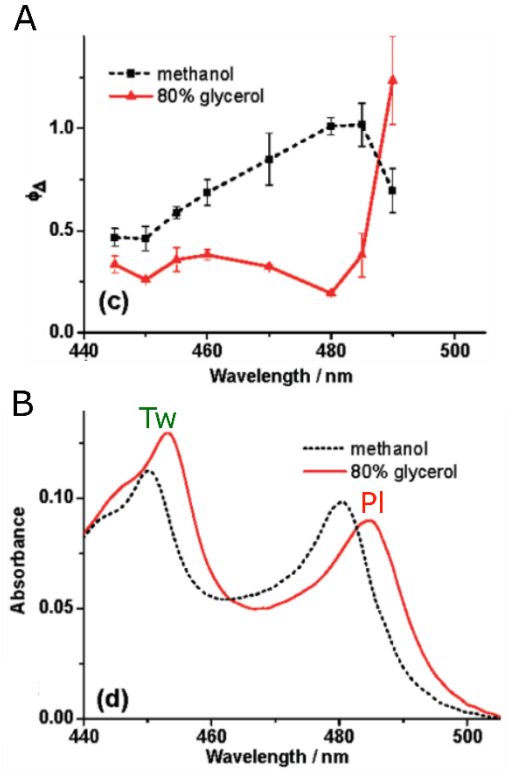

Figure 7. A) Excitation wavelength-dependent quantum yields of singlet oxygen sensitisation of porphyrin dimer **P_2-NMeI** in methanol and in a viscous methanol-glycerol mixture. B) The absorption spectra of the dimer in both solvents. The absorption peaks corresponding to the planar and the twisted conformers are marked. Adapted with permission from Kuimova MK, Balaz M, Anderson HL and Ogilby PR. *J. Am. Chem. Soc.* 2009; **131**: 7948-7949. Copyright 2009 American Chemical Society

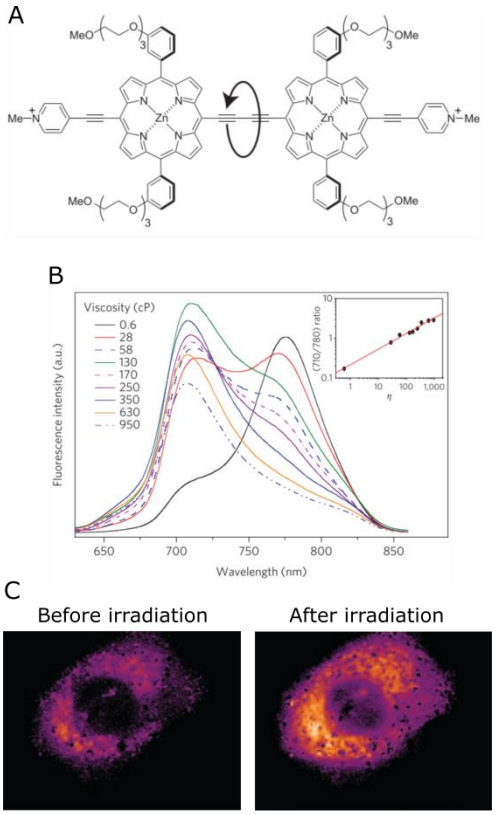

Figure 8. A) A molecular structure of a biocompatible butadiyne-bridged porphyrin dimer **P₂C₂-NMeI**, which was used as a dual agent in live cells: to cause apoptosis as a result of PDT and to measure changes in the intracellular viscosity during photoinduced cell death. B) Fluorescence spectra of **P₂C₂-NMeI** recorded in methanol-glycerol mixtures of varying viscosity. The inset shows the ratiometric calibration curve, based on the twisted *vs* the planar emission peaks' ratio of **P₂C₂-NMeI**. C) Ratiometric fluorescence images (700 ± 20 nm / 800 ± 20 nm) of a single live HeLa cell recorded at the beginning of irradiation and at later stages of apoptosis. Orange colour corresponds to a higher ratio and, hence, a higher intracellular viscosity. Note that the distributions of viscosities in both images are heterogeneous. The figure is adapted from ref.[13] with permission.

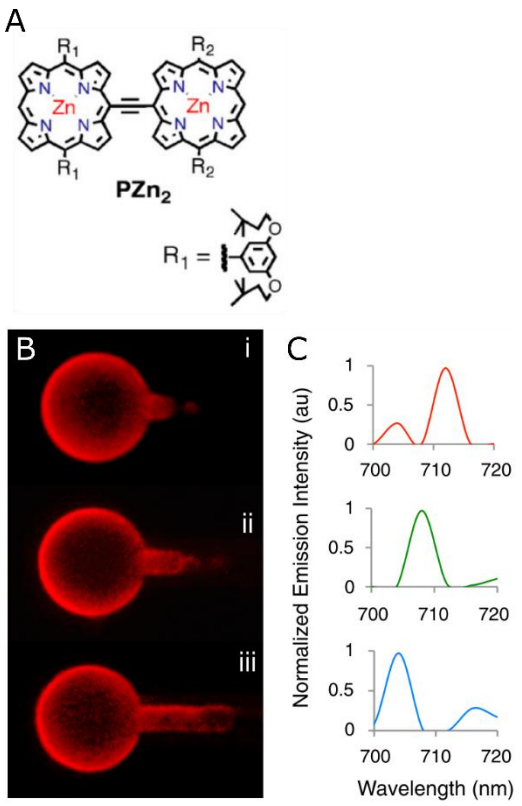

Figure 9. A) A molecular structure of an ethyne-bridged porphyrin dimer **PZn$_2$**, which was used to sense membrane stress in polymersomes during micropipette aspiration. B) Fluorescence images of **PZn$_2$** in polymersomes that are being aspirated with increasing force (i-iii). Fluorescence spectra of **PZn$_2$** are shown in C). The spectrum shifts to lower wavelengths with increasing membrane tension. The figure is adapted from Kamat NP, Liao ZZ, Moses LE, Rawson J, Therien MJ, Dmochowski IJ and Hammer DA. *Proc. Natl. Acad. Sci.* 2011; **108**: 13984-13989 with permission.

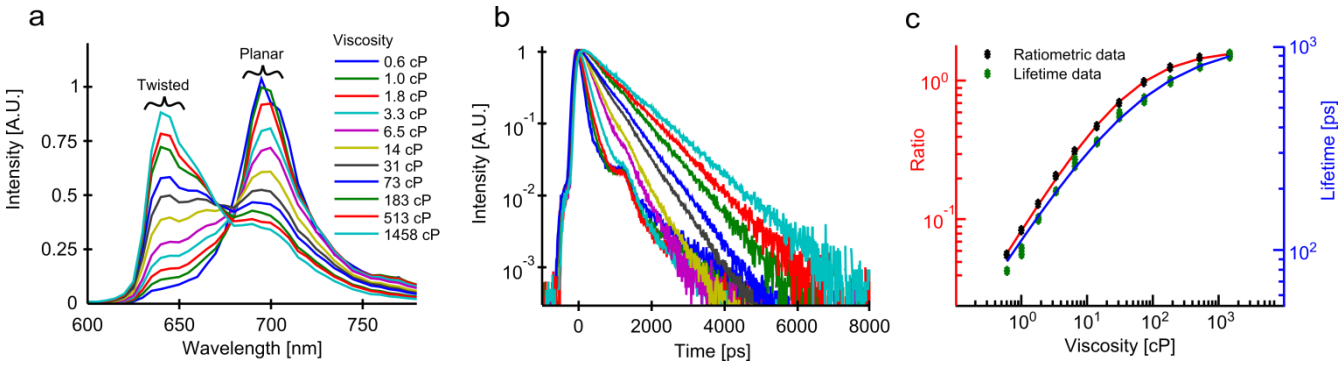

Figure 10. A) Fluorescence spectra of a butadiyne-bridged porphyrin dimer **P$_2$-NMe$_3$OAc** in methanol-glycerol mixtures of varying viscosity. The fluorescence peaks at 640 nm and 710 nm are assigned to the twisted and the planar conformers, respectively. B) The time-resolved fluorescence decays of the twisted conformer at 640 nm in methanol-glycerol mixtures. C) Calibration curves showing the dependences of emission ratio (640 nm / 710 nm) and fluorescence lifetime (640 nm) on viscosity. Both calibration curves show a large dynamic range of values. Reproduced from Ref. 54 with permission from the PCCP Owner Societies.

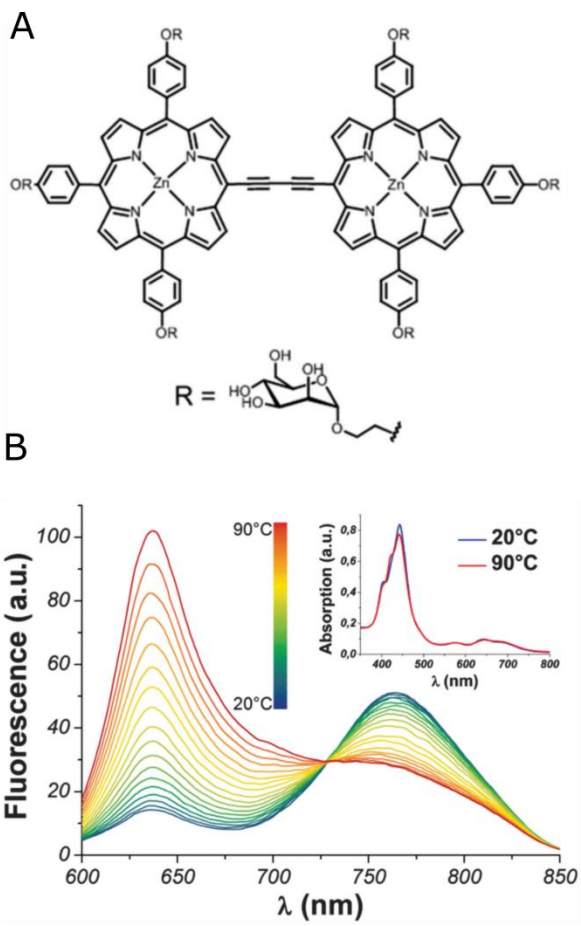

Figure 11. A) A molecular structure of a temperature-sensitive glycosylated porphyrin dimer. B) The fluorescence spectra of the dimer in water recorded at varying temperature. The ratio of the emission intensities at 640 nm and 770 nm increases with increasing temperature. The inset shows an excellent overlap of the dimer's absorption spectra at 20° and 90°C. Reproduced from Ref. 14 with permission from The Royal Society of Chemistry.

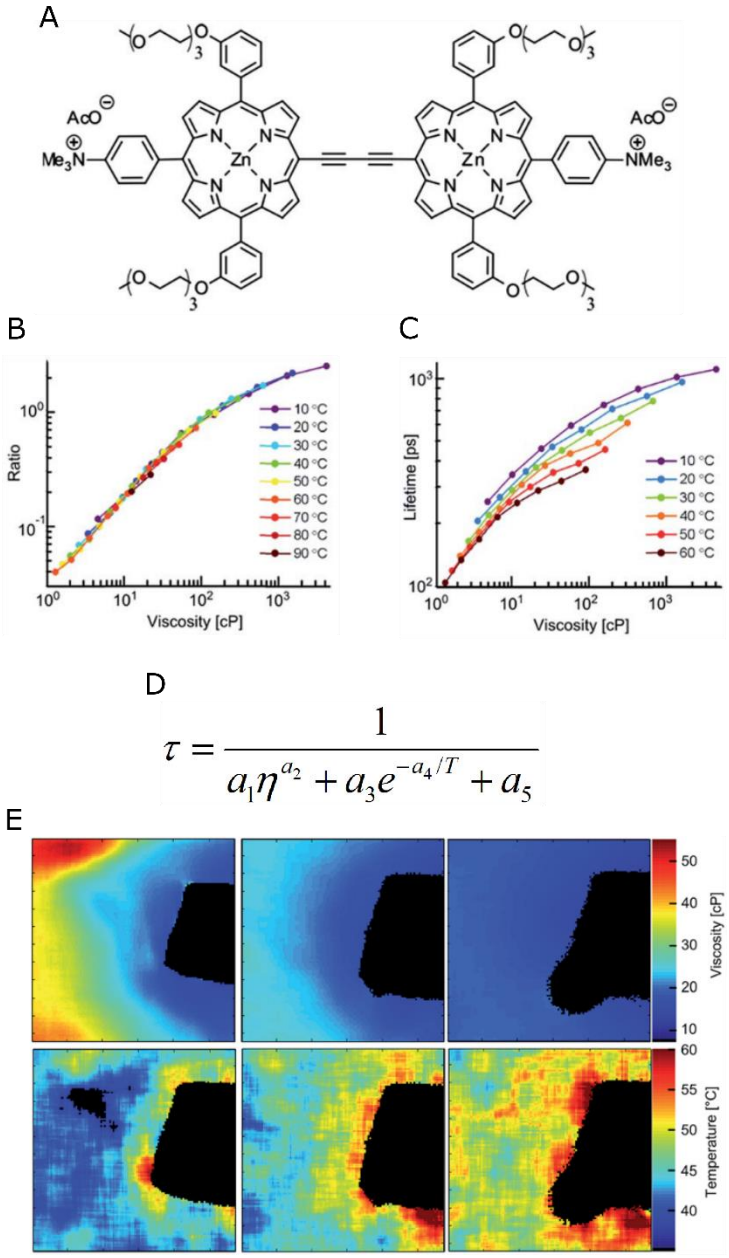

Figure 12. A) A molecular structure of dual viscosity- and temperature-sensitive porphyrin dimer **P_2-NMe_3OAc**. B) The ratiometric calibration plot showing the twisted *vs* the planar conformer emission ratio recorded at varying viscosities and temperatures. The matching viscosities of these solutions (as measured by bulk rheometry) could be achieved by increasing the temperature or lowering the glycerol content. The calibration curves recorded at variable temperature clearly show an excellent overlap, confirming that the viscosity of the solution is the only determinant of the ratio. C) The lifetimes of the twisted conformer recorded at varying viscosities and temperatures. Contrary to the data reported in B, the lifetime-viscosity dependencies are clearly different for different temperatures. D) The function used for fitting viscosity- and temperature-dependent lifetime data shown in C: η is viscosity, T – temperature, $a_{1...5}$ – free flowing fitting parameters. E) Viscosity (top) and temperature (bottom) maps of heated methanol-glycerol mixture under the microscope. The heating was done by a copper wire (black rectangle). The viscosity and temperature images were calculated from simultaneously measured ratiometric and lifetime images, using the calibration shown in B and equation shown in D. Reproduced from Ref. 15 with permission from The Royal Society of Chemistry.

Microviscosity and temperature sensors: the twists and turns of the photophysics of conjugated porphyrin dimers

Aurimas Vyšniauskas, Marina K. Kuimova

Conjugated porphyrin dimers are a class of exciting compounds known for their far-red absorption and emission, high yields of singlet oxygen sensitisation and biocompatibility. Recently it has emerged that porphyrin dimers can also be used for sensing microviscosity and temperature. In this review, we describe the sensing mechanism and demonstrate multiple applications of conjugated porphyrin dimer for sensing microviscosity and temperature in samples raging from solvents to polymers, to live cells.